Cheaper Pre-training Lunch: An Efficient Paradigm for Object Detection

Dongzhan Zhou[1], Xinchi Zhou[1], Hongwen Zhang[2], Shuai Yi[3], and Wanli Ouyang[1]

[1] The University of Sydney, SenseTime Computer Vision Research Group, Australia
{d.zhou,xinchi.zhou1,wanli.ouyang}@sydney.edu.au
[2] Institute of Automation, Chinese Academy of Sciences & University of Chinese Academy of Sciences
hongwen.zhang@cripac.ia.ac.cn
[3] Sensetime Research
yishuai@sensetime.com

Abstract. In this paper, we propose a general and efficient pre-training paradigm, Montage pre-training, for object detection. Montage pre-training needs only the target detection dataset while taking only 1/4 computational resources compared to the widely adopted ImageNet pre-training. To build such an efficient paradigm, we reduce the potential redundancy by carefully extracting useful samples from the original images, assembling samples in a Montage manner as input, and using an ERF-adaptive dense classification strategy for model pre-training. These designs include not only a new input pattern to improve the spatial utilization but also a novel learning objective to expand the effective receptive field of the pre-trained model. The efficiency and effectiveness of Montage pre-training are validated by extensive experiments on the MS-COCO dataset, where the results indicate that the models using Montage pre-training are able to achieve on-par or even better detection performances compared with the ImageNet pre-training.

Keywords: Pre-training, Object Detection, Acceleration, Deep Neural Networks, Deep Learning

1 Introduction

Pre-training on the classification dataset (*e.g.* ImageNet [11]) is a common practice to achieve better network initialization for object detection. Under this paradigm, deep networks benefit from useful feature representations learned from large-scale data, which promotes the convergence of models during fine-tuning stage. Despite the benefits, the burdens caused by extra data should not be neglected.

Previous works [33, 7, 46] have proposed alternative solutions to directly train detection models from scratch with random initialization. However, there is always no free lunch. Training from scratch suffers from slower convergence,

namely, additional training iterations are needed to obtain competitive models. *Can we incorporate the merit of fast convergence via pre-training without paying for the extra data or expensive training cost?*

The answer is **Yes**. We find the cheaper lunch for pre-training. In this work, we propose a new pre-training paradigm, Montage pre-training, which is based only on the detection dataset. Compared with ImageNet pre-training, Montage pre-training takes only 1/4 computational resources without extra data while achieving on-par or even better performance on the target object detection task.

Montage pre-training is built upon the observation that a large number of pixels seen by the model during naive training are invalid or less informative, *i.e.* most pixels/neurons in background regions would not fire during the learning process. Those excessive background pixels inevitably lead to redundant computational costs. To tackle this issue, we carefully extract positive and negative samples from original images in the detection dataset for pre-training. Before being fed into the backbone network, these samples will be assembled in a Montage manner in consideration of their aspect ratios to improve the spatial utilization. To further improve the pixel level utilization, we design an ERF-adaptive dense classification strategy to leverage the Effective Receptive Field (ERF) via assigning soft labels in the learning objective. Our Montage pre-training largely takes every pixel seen by the model into account, which greatly reduces the redundancy and provides an efficient and general pre-training solution for object detection.

Our major contributions can be summarized as follows.

(1) We propose an efficient and general pre-training paradigm based only on detection dataset, which eliminates the burdens of additional data.

(2) We design rules of sample extraction, the Montage assembly strategy, and the ERF-adaptive dense classification for efficient pre-training, which largely considers the network utilization and improves the learning efficiency and final performance.

(3) We validate the effectiveness of our Montage pre-training on various detection frameworks and backbones and demonstrate the versatility of the proposed pre-training strategy. We hope this work would inspire more discussions about the pre-training of object detectors.

2 Related Work

Classification-based Pre-training for Object Detector. Recent years have witnessed the significant breakthroughs of deep learning-based object detectors on various scenarios [5, 17, 27, 31, 8, 1, 23, 20, 25, 45, 38, 22, 18]. Most of these frameworks follow the standard 'pre-training followed by fine-tuning' training procedure, where networks are first pre-trained on the large-scale dataset (*e.g.* ImageNet [11]) and then fine-tuned on the target detection dataset. This pre-training paradigm is mainly classification-based and aims to learn strong or universal representations, which speed up the convergence of detection models. Many efforts have been devoted to push the boundary of transferability further

through different learning modes such as supervised [10], weakly supervised [24, 40], unsupervised [6] learning, or exploiting larger scale training data such as Instagram-17k [24] and JFT-300M [36]. Despite the improvements for transferability, the corresponding expensive training cost of large scale data should not be neglected. Our Montage pre-training is entirely based on detection dataset which eliminates the burden of using external data. Meanwhile, the pre-training process is 4× faster than ImageNet-1k classification training.

Redundancy in Object Detector. Sample imbalance is a common source of redundancy for object detection, where many background pixels belonging to easy negative samples contribute no useful information for training. To alleviate this issue, several attempts have been made to improve the efficiency of detection training. OHEM [34] tries to solve the imbalance sampling by discarding easy negative samples. Focal loss [17] adopts a weighting factor to reduce loss weight for easy samples. Chen *et al.* design a more reasonable method for sample evaluation in [2]. Libra R-CNN [28] proposes the IoU-balanced sampling strategy to augment the hard cases. SNIPER [35] reduces the calculation burden of multi-scale training by only training on selected chips rather than the entire images. All these works mainly focus on the efficiency and performance within detection frameworks, but they still provide inspirations on sample selection in our work. By carefully selecting positive and negative samples for pre-training, the redundancy is significantly reduced, which eventually speeds up the classification pre-training process.

Object Detector Trained from Scratch. Many works [26, 37, 33, 12, 14, 7, 46] have proposed another possible training paradigm which is to train the detector from scratch. For instance, DSOD [33] is motivated by designing a pre-training free detector, but limited to the structure they designed. CornerNet [12] and DetNet [14] present the results of their models trained from scratch. These efforts indicate that pre-training might be unnecessary when adequate data is available. Furthermore, doubts on ImageNet pre-training are also raised recently. He *et al.* [7] and Zhu *et al.* [46] suggest that ImageNet pre-training might be a historical workaround. However, although these solutions get rid of the burdens for large-scale external data, the random initialized detection models suffer from the problem of low convergence speed, which comes at the cost of extending training iterations by 4-5 times to obtain competitive models. Inspired by these works, we move steps forward to exploit an efficient pre-training paradigm for pre-training on detection data, which takes the advantages of both fast convergence and no extra data at the same time.

3 Methodology

The pipeline of using the proposed Montage pre-training scheme is shown in Fig. 1. Given a detection dataset $\mathcal{D}$, positive and negative samples will be extracted from the images of $\mathcal{D}$ and saved as classification dataset beforehand (Sec. 3.1). These samples will be assembled in a Montage manner (Sec. 3.2) and fed into the detector backbone for pre-training, where an ERF-adaptive loss is

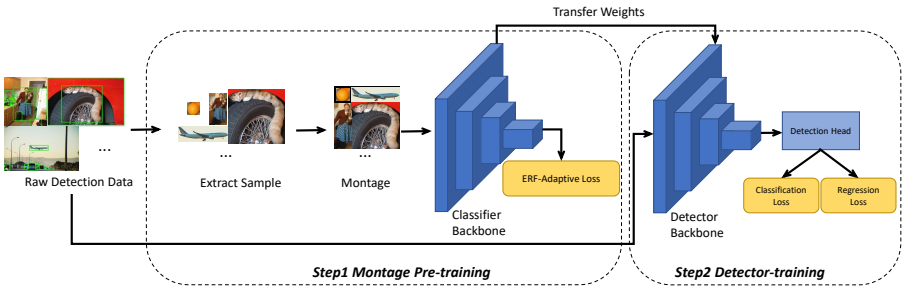

Fig. 1. Pipeline of the proposed Montage pre-training scheme. Firstly, we will extract positive and negative samples from detection data to build classification dataset. The pre-training process is conducted by Montage, which assembles four objects into a single image, and optimized via ERF-adaptive loss. Finally, the backbones will be fine-tuned on target detection task

used as the loss function (Sec. 3.3). After pre-training, the object detector will be fine-tuned on $\mathcal{D}$ under the detection task. Note that our pre-training scheme is flexible and can be applied to object detectors with diverse detection head and backbone architectures.

3.1 Sample Selection

As demonstrated in previous works [34, 28], balanced sample selection is critical during the training of object detectors. For efficient pre-training, we carefully select regions extracted from original images as positive and negative samples, which will be further assembled and fed into the detector backbone.

The positive samples are regions that should be classified as one of the C foreground categories in the detection dataset, while the negative samples are background regions. To effectively select diverse and important samples, we set up following rules for the sample extraction. (1) For **positive samples**, we extract regions from the original images according to the ground-truth bounding boxes. The bounding boxes will be randomly enlarged to involve more context information, which is under the consideration that contextual information is beneficial to learn better feature representations [4, 43]. (2) **Negative samples** are proposals randomly generated from the background regions. To avoid ambiguity, we require that all negative samples meet the requirement $IoU\,(pos, neg) = 0$, where IoU indicates Intersection-over-Union. In our pre-training experiments, the ratio of the number of positive samples to negative ones is $10 : 1$. More details can be found in Section A of the supplementary material.

3.2 Montage Assembly

There are different ways to assemble samples and feed them into the backbone for pre-training. Two straightforward assembling methods are warping (method

1) or padding (method 2) a sample to a pre-defined input size, *e.g.* 224×224. However, forcing all samples to be warped to the same size may destroy the texture information and distort the original shapes, while padding would introduce many uninformative padded pixels and hence bring additional costs in both training time and computational resources. These two straightforward methods are either harmful or wasteful for the pre-training process. For more efficient pre-training, we propose to assemble samples in a Montage manner in consideration of the scale and aspect ratio of objects. Specifically, four samples will be stitched into a new image and then taken as input for pre-training.

As depicted in Fig. 2, compared to warping and padding, our Montage assembly can not only preserve original texture information but also eliminate the uninformative padded pixels.

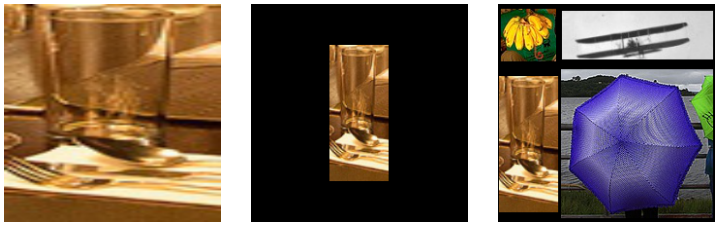

(a) Warping (b) Padding (c) Montage

Fig. 2. Different methods to adjust sample to pre-defined input size. (a) Warping distorts the original shape or texture. (b) Padding introduces many uninformative pixels. (c) Montage preserves original information while improving space utilization

Objects vary in aspect ratio. Montage assembly takes this property into consideration so that samples could be stitched together more naturally according to their aspect ratios. To this end, samples will be first divided into three Groups according to their aspect ratios, *i.e.* Group S (square), T (tall), and W (wide). Samples in Group S should have the aspect ratios between 0.5 and 1.5, while samples in Group T and W should respectively have aspect ratio smaller than 0.5 and larger than 1.5. For simplicity, samples from Group S, T, and W are referred to as S-samples, T-samples, and W-samples, respectively.

As shown in Fig. 3, for every Montage assembled image, 2 S-samples, 1 T-sample, and 1 W-sample will be selected randomly from above three groups and stitched into four regions accordingly. Specifically, the S-sample with smaller bounding box area is at the top-left region, while the larger S-sample is at the bottom-right region. The T-sample and W-sample will be respectively assigned to bottom-left and top-right regions. Details about sample size adjustment (to fit the template) can be found in Section B of the supplementary material.

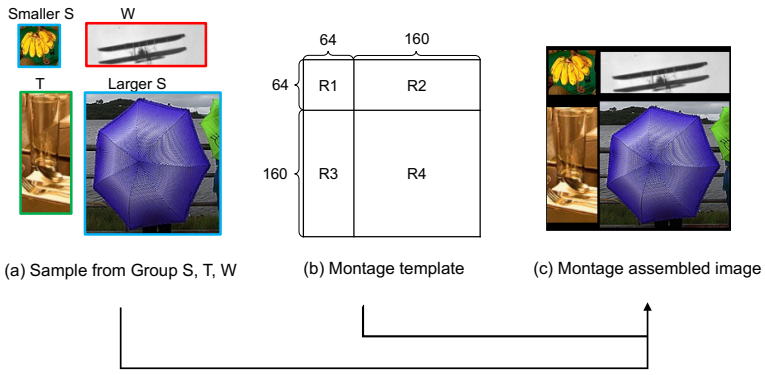

Fig. 3. Pipeline for Montage assembled image generation. We first randomly select 2 S-samples, 1 T-sample and 1 W-sample, respectively as shown in (a), then assemble the samples according to the template (b) and get an assembled image (c). The numbers on Montage template denote the height/width of each region

3.3 ERF-adaptive Dense Classification

During pre-training, the Montage assembled images will be fed into the backbone network to obtain the feature maps $\mathbf{X} \in \mathbb{R}^{C\times\alpha H\times\alpha W}$ before the final average pooling. Here we omit the number of samples in $\mathbf{X}$ for simplicity. Compared to the conventional classification pre-training, Montage pre-training should have different learning strategy since there are four samples stitched in one assembled image. In the following, we discuss two alternative strategies and then introduce our proposed ERF-adaptive Dense Classification.

Global classification. As shown in Fig. 3, an image contains four objects in our Montage assembled image. As an intuitive strategy, we can assign the whole image a single global label, which is the weighted sum of the labels of the four objects according to their region areas. This strategy could be reminiscent of the CutMix [42], where certain region of the original image will be replaced by a patch from another image and the corresponding label will also be mixed proportionally with the label of the new patch. The visualization of global classification will be provided in the supplementary material.

Block-wise classification. Another intuitive strategy would perform individually for each block/region, that is, the average pooling is independently applied to the four blocks of feature maps $\mathbf{X}$ corresponding to four samples, followed by individual classification according to the label of each sample. However, these two intuitive strategies confine the learning of each block to the corresponding sample. As can be seen in Fig. 5(a) and 5(b), the Effective Receptive Field (ERF) [21] of the top-left region in $\mathbf{X}$ mainly concentrates on the area of the corresponding smaller S-sample. The confined receptive field may empircally degrade the performance of deep models, as illustrated in [19, 13, 30]. The visualization of block-wise classification will be provided in the supplementary material.

Our strategy. To largely take every seen pixel into account, we propose an ERF-adaptive Dense Classification strategy to perform classification for each position at $\mathbf{X}$, where its soft labels are computed based on the corresponding effective receptive field. The process is depicted in Fig. 4.

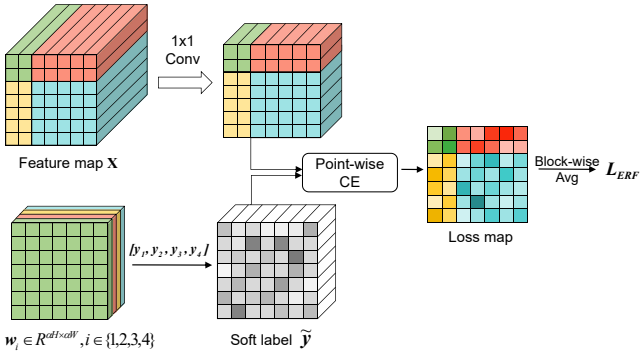

Fig. 4. Process of our Dense Classification Strategy. We use different colors to distinguish different regions, *e.g.* green for R_1, and the brightness difference in soft label and loss map represents different values. The feature map $\mathbf{X}$ is convolved by a 1×1 kernel to reduce the number of channels to C (category number). Given the weight w_i of label $\mathbf{y_i}$, we obtain the soft label tensor for each point. Then the cross-entropy loss is densely imposed on the feature map and we will get the loss value at each point (denoted as loss map). In the mean time, the loss weight for a position is calculated according to the ERF of the position. After that, block-wise average is exerted on the loss map to generate average losses for each region. The final ERF-adaptive loss is the mean of four region losses. Best viewed in color

Specifically, for the four regions in the Montage template as shown in Fig. 3(b), we denote $\mathbf{y}_i$ as the original label for the region R_i, $i = 1, 2, 3, 4$.

At the position (j, k) of feature map $\mathbf{X}$ ($j = 1, \ldots, \alpha H, k = 1, \ldots, \alpha W$), the soft label $\tilde{\mathbf{y}}^{j,k}$ is the weighted sum of four labels:

$$\tilde{\mathbf{y}}^{j,k} = \sum_{i=1}^{4} w_i^{j,k} \mathbf{y}_i, \tag{1}$$

where the weight $w_i^{j,k}$ is dependent on its ERF. At the position (j, k) of feature map $\mathbf{X}$ ($j = 1, \ldots, \alpha H, k = 1, \ldots, \alpha W$), we obtain the corresponding ERF $\mathbf{G}^{j,k} \in \mathbb{R}^{H \times W}$ on the input space. Then, the weight $w_i^{j,k}$ for the label $\mathbf{y}_i$ at position (j, k) should be proportional to the ratio of the summed activation within the region R_i to the whole summed activation. Moreover, if the position (j, k) is in region R_i, we empirically set a threshold τ for $w_i^{j,k}$ to make sure that $\mathbf{y}_i$ is dominant at region R_i. Hence, for the position (j, k) at region R_r, we have the weight $w_i^{j,k}$ of the label $\mathbf{y}_i$ as follows:

$$w_i^{j,k} = \begin{cases} \max(\tau, \frac{\sum_{h=1,w=1}^{H,W} g_{h,w}^{j,k} \cdot m_{h,w}^i}{\sum_{h=1,w=1}^{H,W} g_{h,w}^{j,k}}), \text{if } i = r, \\ (1 - w_r^{j,k}) \frac{\sum_{h=1,w=1}^{H,W} g_{h,w}^{j,k} \cdot m_{h,w}^i}{\sum_{h=1,w=1}^{H,W} g_{h,w}^{j,k} \cdot (1 - m_{h,w}^r)}, \text{if } i \neq r, \end{cases} \tag{2}$$

where $g_{h,w}^{j,k}$ is the element at position (h, w) on the corresponding ERF matrix $\mathbf{G^{j,k}}$, $m_{h,w}^i$ refers to the value at position (h, w) on binary mask $\mathbf{M}^i \in \{0, 1\}^{H \times W}$. The binary mask $\mathbf{M}^i$ is used to select the region R_i in ERF.

Denote $\mathbf{x}^{j,k} \in \mathbb{R}^C$ as the features at the position (j, k) of $\mathbf{X}$ ($j = 1, \ldots, \alpha H, k = 1, \ldots, \alpha W$). After obtaining the weights $\{w_i^{j,k}\}_{i=1}^4$, we perform dense classification upon the feature $\mathbf{x}^{j,k}$, where its soft label $\tilde{\mathbf{y}}^{j,k}$ is defined in Eq. (1). In our implementation, the final fully connected layer is replaced by a 1×1 convolution layer and the cross-entropy loss is imposed on the category prediction at every position. To make a balance among different regions, the final ERF-adaptive loss is the block-wise average of the loss map, as the last step in Fig. 4. We also need to clarify that the weights of soft label Eq. (1) are updated at every 5k iterations instead of at each iteration. Thus, even if dense classification is adopted, its effect on training time is negligible. Correspondingly, since ERF will be updated regularly during the whole training process, different initialization choices of ERF will not affect the final results. We choose the method to calculate ERF based on the randomly initialized network parameters.

The effective receptive field of the top-left region for the different pre-training strategies is visualized in Fig. 5. Our strategy in Fig. 5(c) has the largest ERF among the above three strategies.

Relationships among Different Strategies. The above three strategies perform classification at different scale levels, where the proposed ERF-adaptive classification is the most fine-grained one while the global classification is the coarsest one. Compared with the other two alternative strategies, the proposed one has different soft labels for each position at $\mathbf{X}$. The ERF-adaptive dense classification would be equivalent to the block-wise classification with threshold τ set to 1. The block-wise classification would be also equivalent to the global classification if the region losses are re-weighted in a CutMix manner. Under different label assignment strategies, the pre-trained model has different pixel level utilization and hence behaves differently. Comparison of performance for the strategies can be found in the supplementary material.

4 Experiments

4.1 Implementation details

This section introduces the implementation details of the classification pre-training. Details of data augmentation in pre-training and detector training settings will be provided in the supplementary.

Unless otherwise specified, the models are pre-trained for 64k iterations on 8 Tesla V100 GPUs with the total batch size of 512. Note that the batch size 512

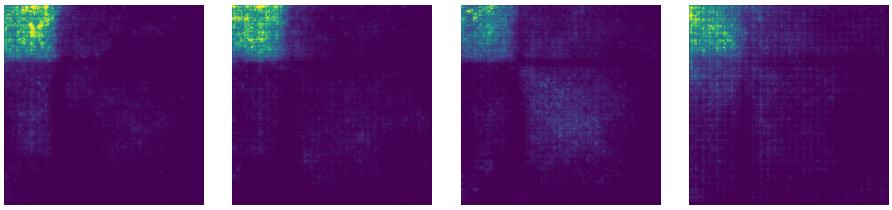

(a) Global (b) Block-wise (c) ERF-adaptive (d) ImageNet

Fig. 5. Visualization of Effective Receptive Field of the top-left region for different pre-trained models. (a) Global represents conducting global average pooling and set global label as weighted sum of labels from four regions. (b) Block-wise refers to the intuitive strategy which performs classification individually on each region. (c) ERF-adaptive refers to adopting ERF-adaptive dense classification. (d) ImageNet stands for the ImageNet pre-trained model officially provided by PyTorch [29]

is for Montage assembled images, so the total number of individual samples in each batch is 2048 (an assembled image consists of 4 samples). Warm-up is used during the first 1250 iterations, where the learning rate starts from 0.2 and then linearly increases to 0.8. Afterwards, the learning rate decreases to 0.0 following a cosine scheduler. The weight decay is 1e−4. We update weights $w_i^{j,k}$ of soft labels in Eq. 2 for every 5k iterations. The threshold τ in Eq. 2 for ERF-adaptive classification is set to 0.7. The data augmentation implementation can be found in the supplementary.

4.2 Main Results

We conduct the Montage pre-training process based on samples extracted from MS-COCO train2017 split, and fine-tune the detection models on the same dataset. The backbone is ResNet-50. Note that the Montage pre-training process only consumes **1/4** computation resources compared with ImageNet pre-training. As reported in Table 1, the results show that the models using our Montage pre-training strategy are able to achieve on-par or even better performances compared with the ImageNet pre-training counterparts for various detection frameworks. For original Faster R-CNN [32], the AP increases from 34.8% to 36.3% (+1.5%), for Faster R-CNN with FPN [16], AP increases from 36.2% to 36.5% (+0.3%), for Mask R-CNN with FPN [8], AP increases from 37.2% to 37.4%(+0.2%).

We notice that the improvement is most significant in the original Faster R-CNN structure (denoted as C4 in Table 1). We suspect the possible reason is that, compared with FPN structure, the backbone accounts for a larger proportion in C4. In other words, for detection models with FPN structure, the lateral connections and entire structures at the second stage will be randomly initialized without being transferred from pre-trained model. But for the original Faster R-CNN, the main part of the second stage is still transferred from the pre-trained

network. We speculate that the improvement of detection models with FPN may be consistent with that of C4 if the FPN structure is incorporated into pre-training, and we will leave this exploration for future work.

Table 1. Results on different detection frameworks with backbone ResNet-50. The cost refers to pre-training cost and the unit is GPU days. The AP results are evaluated on COCO val2017. 'C4' denotes original Faster R-CNN without FPN [32], 'FPN' denotes Faster R-CNN with FPN [16], 'Mask' denotes Mask R-CNN with FPN [8]. '+ ImageNet' means the backbone is pre-trained on ImageNet dataset. '+ Montage' denotes that the backbone is pre-trained with our Montage strategy. Δ measures the difference in absolute AP or cost between adopting Montage and ImageNet pre-trained backbones, respectively

Method	Cost	AP	AP_{50}	AP_{75}	AP_s	AP_m	AP_l
C4[32] + ImageNet	6.80	34.8	55.5	36.8	18.3	38.7	48.4
C4[32] + Montage	1.73	36.3	56.5	38.9	18.9	40.8	49.7
Δ	-5.07	+1.5	+1.0	+2.1	+0.6	+2.1	+1.3
FPN[16] + ImageNet	6.80	36.2	58.0	39.2	21.2	39.9	45.6
FPN[16] + Montage	1.73	36.5	58.3	39.2	22.2	40.4	45.8
Δ	-5.07	+0.3	+0.3	0.0	+1.0	+0.5	+0.2
Mask[8] + ImageNet	6.80	37.3	59.0	40.3	21.9	40.6	46.2
Mask[8] + Montage	1.73	37.5	58.9	40.6	22.8	41.2	46.9
Δ	-5.07	+0.2	-0.1	+0.3	+0.9	+0.6	+0.7

4.3 Ablation study

Threshold for ERF-adaptive Dense Classification. When ERF-adaptive Dense Classification is used, there is a threshold τ in Eq. (1) to make sure that the original label y_i is dominant at its corresponding region i. We explore the effects of this threshold and the results are depicted in Fig. 6(a). Although using mixed labels is beneficial, relatively low proportion of original label (*e.g.* 0.5) may still hinder the pre-training. As the threshold becomes higher, the loss is gradually approaching the use of single hard label for each point, which may suffer from relatively confined receptive field, as analyzed in Section 3.3. Therefore, it is important to choose proper threshold and we find 0.7 is an ideal choice. Fig. 6(a) also shows that setting the threshold in [0.6 0.8] will not cause much variation in mAP. Therefore, the experimental results are not so sensitive to this hyper-parameter.

Iterations for pre-training. We also investigate the influences of changing the pre-training iterations and visualize the results in Fig. 6(b). Naturally, increasing training iterations will provide better pre-trained models, which leads to better detection performance. But we also observe that the gains from longer iterations are not so significant after 64k iterations (4× in Fig. 6(b)). Considering the trade-off between performance and computation, we choose to train 64k iterations

during pre-training, which consumes only 1/4 computation resources but achieve 1.5% higher mAP compared with ImageNet pre-training.

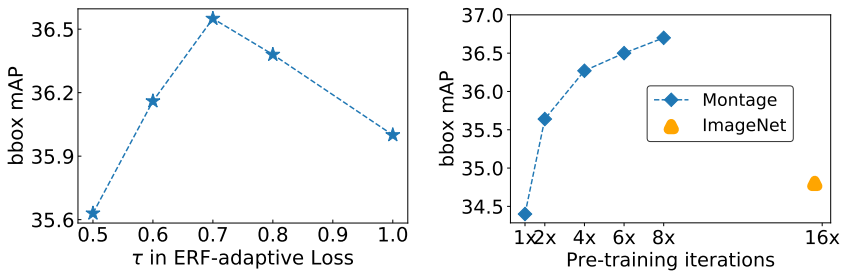

Fig. 6. (a) Trend of bbox mAP with different τ settings in ERF-adaptive loss. (b) bbox mAP for different pre-training iterations, the values on x-axis stand for multiple of 16k iterations. Our pre-training approach uses $4\times$ as the default setting, which requires 1/4 the number of iterations but achieves 1.5% higher mAP when compared with ImageNet counterpart. The results are evaluated on COCO val2017

Different backbone structures. We also implement our pre-training strategy on different backbone structures to evaluate the versatility. The results in Table 2 show that Montage pre-training strategy does not rely on specific network structures but will consistently keep on-par performance or obtain improvements.

Table 2. Results for different backbone structures evaluated on COCO val2017. The detection framework is original Faster R-CNN. ImageNet means the backbone is trained on ImageNet dataset. Montage denotes that the backbone is pre-trained with Montage strategy. X101-32x4d refers to ResNeXt101-32x4d [41]

Method	AP	AP_{50}	AP_{75}	AP_s	AP_m	AP_l
ResNet-101 + ImageNet	38.3	58.9	41.1	20.0	42.8	53.0
ResNet-101 + Montage	39.2	59.6	42.0	20.6	43.3	54.8
Δ	+0.9	+0.7	+0.9	+0.6	+0.5	+1.8
X101-32x4d + ImageNet	40.2	61.2	43.2	21.2	44.6	55.7
X101-32x4d + Montage	40.2	61.0	43.0	21.3	44.5	55.7
Δ	0.0	-0.2	-0.2	+0.1	-0.1	0.0

4.4 Compatibility to other designs

We also examine the compatibility of Montage pre-training strategy with commonly used designs in object detection, including longer training iterations (2x

schedule), deformable convolution [3], multi-scale augmentation, etc. The results in Fig. 7 indicate that Montage pre-training can still achieve comparable or even higher performance even on various enhanced baselines.

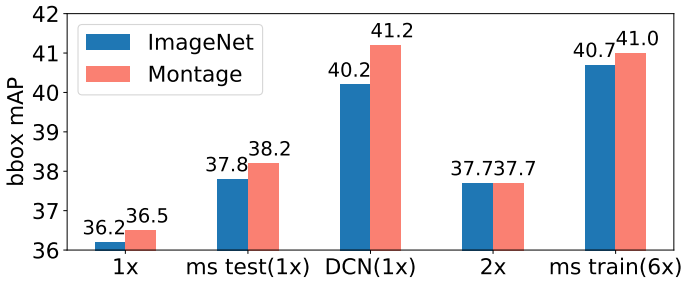

Fig. 7. Comparison between **ImageNet** pre-training and **Montage** pre-training of various strategies on Faster R-CNN FPN framework with ResNet-50 backbone, the results are evaluated on COCO val2017. Strategies include: (1) 1×: serving as original strategy that train for 1× schedule (13 epochs), (2) ms test: adding multi-scale augmentation during test stage, (3) DCN: replace the 3×3 convolution layers of stage 2-4 in backbone with 3×3 deformable convolution layer [3], (4) 2×: extending the training time to 2× schedule, (5) ms train: implementing multi-scale augmentation during train and test stage and extending training epochs to 6× schedule

It is worth noting that the most obvious improvement has been achieved when replacing some convolution layers to deformable convolution layers. We suspect that this improvement may come from the relief of domain shift between pre-training dataset and detection dataset. Therefore, our approach has the potential of further boosting the performance gains from new designs on backbones.

4.5 Comparison with vanilla training detection from scratch

We also compare our Montage pre-training strategy with the vanilla training detection from scratch method (denoted as **vanilla scratch** for simplicity). Vanilla scratch and our strategy share an advantage that the entire training process is only based on detection dataset without introducing any external data. However, adopting pre-training process will speed up the convergence of detection models, which helps the models achieve better performance under common training iterations, such as 1× or 2× schedules. The results are presented in Table 3. To make a fair comparison, we keep total training costs similar for the two methods, that is, the total costs in our method include both pre-training and detection training consumptions. We follow the experimental settings for vanilla scratch in [7] where all batch norm layers in the network are replaced by group norm [39]. The batch norm layers are frozen at detection stage when transferring from our pre-trained backbones. The results indicate that even with group normalization,

which is proven to improve the performance of detection models, vanilla scratch still shows suboptimal performance compared with our pre-training strategy.

Table 3. Comparison of vanilla scratch and Montage pre-training under similar computation costs. The detection framework is Faster R-CNN with backbone ResNet-50, and the AP results are evaluated on COCO val2017. The unit for total cost is GPU days. 1× refer to training detection models for widely adopted 1× schedule, while 2× to extend the iterations to twice

Method	Total Cost	AP	AP_{50}	AP_{75}
Vanilla scratch	6.0	28.6	46.5	30.1
Montage + 1×	5.8	36.3	56.5	38.9
Vanilla scratch	9.5	32.6	51.6	34.7
Montage + 2×	9.2	37.5	57.6	40.7

5 Discussion

The possible reasons for the Montage pre-training being effective are as follows:

First, there is domain gap between the ImageNet dataset and objective detection dataset, such as the data distribution and category. Directly pre-training on the target detection dataset will alleviate the domain gap and help obtain better initialization. However, simply changing the pre-training dataset is not enough and the specially designed pre-training strategy is necessary. Table 4 shows the comparison between simply replacing dataset from ImageNet to MS-COCO and Montage pre-training. We can see that pre-training on MS-COCO classification for the same training time as ours (1.73 GPU days) performs worse than ImageNet classification and our approach. Thus, directly training on MS-COCO by saving the training computational costs leads to drop in detection accuracy. If the training time on MS-COCO is extended to the same as that on ImageNet (6.80 GPU days), the final AP will be similar to ImageNet, but still worse than our approach. Therefore, preserving detection accuracy and saving computational cost at the same time cannot be simply brought by adopting MS-COCO classification dataset, but our Montage pre-training strategy is able to preserve detection performance under lower computation costs.

Second, we speculate that the improved training efficiency of Montage pre-training comes from the reduction of redundancy in training dataset. In the training dataset, the amount of foreground and background pixels are imbalanced, especially for the detection dataset. Thus, we design a reasonable sampling strategy to compose training data, which makes the pre-trained networks focus more on positive samples. By discarding the useless pixels and effectively assembling training samples, our Montage pre-training strategy contributes to the reduction of redundancy, which explains the improvements of training effi-

Table 4. Experimental results on ImageNet pre-training, Montage Pre-training using the same and higher computational costs. The detection framework is Faster R-CNN with backbone ResNet50, and the AP results are evaluated on COCO val2017. The unit of cost is GPU days. ImageNet refers to pre-training on ImageNet dataset and MS-COCO represents training on samples extracted from MS-COCO dataset, as illustrated in Section 3.1

Method	Total Cost	AP
ImageNet	6.80	34.8
MS-COCO *w/o* Montage (higher cost)	6.80	34.4
MS-COCO *w/o* Montage	1.73	33.5
MS-COCO *w.* Montage (ours)	1.73	36.3

ciency. By assigning soft labels at the regions that overlap with multiple objects leads, more supervised signals are provided for learning better features.

Finally, the ERF-adaptive loss has positive effects on expanding the effective receptive field of the pre-trained models, which provides stronger supervision signals and obtains pre-trained model more appropriate for the detection task. Larger receptive field helps to promote the performance of detection models, as demonstrated in previous works [13, 19, 3].

6 Conclusions

In this work, we present a choice to obtain cheaper lunch on pre-training for object detection, which is able to reduce the consumption of pre-training to 1/4 compared with the original ImageNet pre-training, while achieving on-par or even higher performance. We define a novel pre-training paradigm based only on detection dataset, which eliminates the burdens of extra training data while retaining the advantage of fast convergence. Our efficient Montage Pre-training facilitates training from scratch, which can reduce the computational cost when directly using network compression and neural architecture search [44, 9] for target tasks like object detection. We expect this work would help researchers reduce the trial-and-error cost, inspire more future research on pre-training process, and facilitate new backbone CNN architecture design/search [15] tailored for object detection.

Acknowledgement This work was supported by SenseTime, the Australian Research Council Grant DP200103223, and Australian Medical Research Future Fund MRFAI000085.

References

1. Brazil, G., Liu, X.: M3d-rpn: Monocular 3d region proposal network for object detection. In: The IEEE International Conference on Computer Vision (ICCV) (October 2019)
2. Chen, K., Li, J., Lin, W., See, J., Wang, J., Duan, L., Chen, Z., He, C., Zou, J.: Towards accurate one-stage object detection with ap-loss. In: Proceedings of the IEEE Conference on Computer Vision and Pattern Recognition. pp. 5119–5127 (2019)
3. Dai, J., Qi, H., Xiong, Y., Li, Y., Zhang, G., Hu, H., Wei, Y.: Deformable convolutional networks. In: Proceedings of the IEEE international conference on computer vision. pp. 764–773 (2017)
4. Divvala, S.K., Hoiem, D., Hays, J.H., Efros, A.A., Hebert, M.: An empirical study of context in object detection. In: 2009 IEEE Conference on computer vision and Pattern Recognition. pp. 1271–1278. IEEE (2009)
5. Girshick, R., Donahue, J., Darrell, T., Malik, J.: Rich feature hierarchies for accurate object detection and semantic segmentation. In: Proceedings of the IEEE conference on computer vision and pattern recognition. pp. 580–587 (2014)
6. He, K., Fan, H., Wu, Y., Xie, S., Girshick, R.: Momentum contrast for unsupervised visual representation learning. arXiv preprint arXiv:1911.05722 (2019)
7. He, K., Girshick, R., Dollár, P.: Rethinking imagenet pre-training. In: Proceedings of the IEEE International Conference on Computer Vision. pp. 4918–4927 (2019)
8. He, K., Gkioxari, G., Dollár, P., Girshick, R.: Mask r-cnn. In: Proceedings of the IEEE international conference on computer vision. pp. 2961–2969 (2017)
9. Jiang, C., Xu, H., Zhang, W., Liang, X., Li, Z.: Sp-nas: Serial-to-parallel backbone search for object detection. In: Proceedings of the IEEE/CVF Conference on Computer Vision and Pattern Recognition. pp. 11863–11872 (2020)
10. Kornblith, S., Shlens, J., Le, Q.V.: Do better imagenet models transfer better? In: Proceedings of the IEEE conference on computer vision and pattern recognition. pp. 2661–2671 (2019)
11. Krizhevsky, A., Sutskever, I., Hinton, G.E.: Imagenet classification with deep convolutional neural networks. In: Advances in neural information processing systems. pp. 1097–1105 (2012)
12. Law, H., Deng, J.: Cornernet: Detecting objects as paired keypoints. In: Proceedings of the European Conference on Computer Vision (ECCV). pp. 734–750 (2018)
13. Li, Y., Chen, Y., Wang, N., Zhang, Z.: Scale-aware trident networks for object detection. In: Proceedings of the IEEE International Conference on Computer Vision. pp. 6054–6063 (2019)
14. Li, Z., Peng, C., Yu, G., Zhang, X., Deng, Y., Sun, J.: Detnet: A backbone network for object detection. arXiv preprint arXiv:1804.06215 (2018)
15. Liang, F., Lin, C., Guo, R., Sun, M., Wu, W., Yan, J., Ouyang, W.: Computation reallocation for object detection. arXiv preprint arXiv:1912.11234 (2019)
16. Lin, T.Y., Dollár, P., Girshick, R., He, K., Hariharan, B., Belongie, S.: Feature pyramid networks for object detection. In: Proceedings of the IEEE conference on computer vision and pattern recognition. pp. 2117–2125 (2017)
17. Lin, T.Y., Goyal, P., Girshick, R., He, K., Dollár, P.: Focal loss for dense object detection. In: Proceedings of the IEEE international conference on computer vision. pp. 2980–2988 (2017)
18. Liu, L., Ouyang, W., Wang, X., Fieguth, P., Chen, J., Liu, X., Pietikäinen, M.: Deep learning for generic object detection: A survey. International journal of computer vision **128**(2), 261–318 (2020)

19. Liu, S., Huang, D., et al.: Receptive field block net for accurate and fast object detection. In: Proceedings of the European Conference on Computer Vision (ECCV). pp. 385–400 (2018)
20. Lu, X., Li, B., Yue, Y., Li, Q., Yan, J.: Grid r-cnn. In: Proceedings of the IEEE Conference on Computer Vision and Pattern Recognition. pp. 7363–7372 (2019)
21. Luo, W., Li, Y., Urtasun, R., Zemel, R.: Understanding the effective receptive field in deep convolutional neural networks. In: Advances in neural information processing systems. pp. 4898–4906 (2016)
22. Ma, X., Liu, S., Xia, Z., Zhang, H., Zeng, X., Ouyang, W.: Rethinking pseudo-lidar representation. In: Proceedings of the European Conference on Computer Vision (ECCV) (2020)
23. Ma, X., Wang, Z., Li, H., Zhang, P., Ouyang, W., Fan, X.: Accurate monocular 3d object detection via color-embedded 3d reconstruction for autonomous driving. In: Proceedings of the IEEE/CVF International Conference on Computer Vision (ICCV) (October 2019)
24. Mahajan, D., Girshick, R., Ramanathan, V., He, K., Paluri, M., Li, Y., Bharambe, A., van der Maaten, L.: Exploring the limits of weakly supervised pretraining. In: Proceedings of the European Conference on Computer Vision (ECCV). pp. 181–196 (2018)
25. Manhardt, F., Kehl, W., Gaidon, A.: Roi-10d: Monocular lifting of 2d detection to 6d pose and metric shape. In: The IEEE Conference on Computer Vision and Pattern Recognition (CVPR) (June 2019)
26. Matan, O., Burges, C.J., LeCun, Y., Denker, J.S.: Multi-digit recognition using a space displacement neural network. In: Advances in neural information processing systems. pp. 488–495 (1992)
27. Ouyang, W., Wang, K., Zhu, X., Wang, X.: Chained cascade network for object detection. In: Proceedings of the IEEE International Conference on Computer Vision. pp. 1938–1946 (2017)
28. Pang, J., Chen, K., Shi, J., Feng, H., Ouyang, W., Lin, D.: Libra r-cnn: Towards balanced learning for object detection. In: Proceedings of the IEEE Conference on Computer Vision and Pattern Recognition. pp. 821–830 (2019)
29. Paszke, A., Gross, S., Massa, F., Lerer, A., Bradbury, J., Chanan, G., Killeen, T., Lin, Z., Gimelshein, N., Antiga, L., et al.: Pytorch: An imperative style, high-performance deep learning library. In: Advances in Neural Information Processing Systems. pp. 8024–8035 (2019)
30. Peng, J., Sun, M., ZHANG, Z.X., Tan, T., Yan, J.: Efficient neural architecture transformation search in channel-level for object detection. In: Advances in Neural Information Processing Systems. pp. 14290–14299 (2019)
31. Redmon, J., Divvala, S., Girshick, R., Farhadi, A.: You only look once: Unified, real-time object detection. In: Proceedings of the IEEE conference on computer vision and pattern recognition. pp. 779–788 (2016)
32. Ren, S., He, K., Girshick, R., Sun, J.: Faster r-cnn: Towards real-time object detection with region proposal networks. In: Advances in neural information processing systems. pp. 91–99 (2015)
33. Shen, Z., Liu, Z., Li, J., Jiang, Y.G., Chen, Y., Xue, X.: Dsod: Learning deeply supervised object detectors from scratch. In: Proceedings of the IEEE international conference on computer vision. pp. 1919–1927 (2017)
34. Shrivastava, A., Gupta, A., Girshick, R.: Training region-based object detectors with online hard example mining. In: Proceedings of the IEEE conference on computer vision and pattern recognition. pp. 761–769 (2016)

35. Singh, B., Najibi, M., Davis, L.S.: Sniper: Efficient multi-scale training. In: Advances in neural information processing systems. pp. 9310–9320 (2018)
36. Sun, C., Shrivastava, A., Singh, S., Gupta, A.: Revisiting unreasonable effectiveness of data in deep learning era. In: Proceedings of the IEEE international conference on computer vision. pp. 843–852 (2017)
37. Szegedy, C., Toshev, A., Erhan, D.: Deep neural networks for object detection. In: Advances in neural information processing systems. pp. 2553–2561 (2013)
38. Tan, M., Pang, R., Le, Q.V.: Efficientdet: Scalable and efficient object detection. arXiv preprint arXiv:1911.09070 (2019)
39. Wu, Y., He, K.: Group normalization. In: Proceedings of the European Conference on Computer Vision (ECCV). pp. 3–19 (2018)
40. Xie, Q., Hovy, E., Luong, M.T., Le, Q.V.: Self-training with noisy student improves imagenet classification. arXiv preprint arXiv:1911.04252 (2019)
41. Xie, S., Girshick, R., Dollár, P., Tu, Z., He, K.: Aggregated residual transformations for deep neural networks. In: Proceedings of the IEEE conference on computer vision and pattern recognition. pp. 1492–1500 (2017)
42. Yun, S., Han, D., Oh, S.J., Chun, S., Choe, J., Yoo, Y.: Cutmix: Regularization strategy to train strong classifiers with localizable features. In: The IEEE International Conference on Computer Vision (ICCV) (October 2019)
43. Zheng, W.S., Gong, S., Xiang, T.: Quantifying and transferring contextual information in object detection. IEEE transactions on pattern analysis and machine intelligence **34**(4), 762–777 (2011)
44. Zhou, D., Zhou, X., Zhang, W., Loy, C.C., Yi, S., Zhang, X., Ouyang, W.: Econas: Finding proxies for economical neural architecture search. In: Proceedings of the IEEE/CVF Conference on Computer Vision and Pattern Recognition. pp. 11396–11404 (2020)
45. Zhu, C., He, Y., Savvides, M.: Feature selective anchor-free module for single-shot object detection. In: Proceedings of the IEEE Conference on Computer Vision and Pattern Recognition. pp. 840–849 (2019)
46. Zhu, R., Zhang, S., Wang, X., Wen, L., Shi, H., Bo, L., Mei, T.: Scratchdet: Training single-shot object detectors from scratch. In: Proceedings of the IEEE conference on computer vision and pattern recognition. pp. 2268–2277 (2019)